Table V. Dimensions of Some Aryldiazo Complexes from X-ray Diffraction Studies

compd	M-N, Å	N-N, Å	N-C, Å	M-N-N, deg	N-N-C, deg	ref
		Singly Bent				
$Mo(N_2Ph)(dtc)_3$	1.781 (4)	1.233 (6)	1.417 (7)	171.5 (4)	120.5 (5)	4b
$[HB(pz)_3]Mo(CO)_2(N_2Ph)$	1.825 (4)	1.211 (6)	1.432 (7)	174.2 (1)	121.1 (2)	3d
$[IrCl(N_2Ph)(PPh_3)_2]^+$	1.794	1.159	1.45	176.1	126	3a
$Ru(p\text{-}N_2C_6H_4CH_3)Cl_3(PPh_3)_2$	1.796 (9)	1.144 (10)	1.40	171.2 (9)	135.9 (11)	3e
$Re(N_2Ph)Cl_2(PMe_2Ph)_3$	1.80 (1)	1.23 (1)		172	118	4a
		Doubly Bent				
$[Rh(N_2Ph)Cl(PPP)]^+$ [a]	1.961 (7)	1.172 (9)	1.445 (11)	125.1 (6)	118.9 (8)	3f
$PtCl(p\text{-}N_2C_6H_4F)(PEt_3)_2$	1.975 (28)	1.17 (3)	1.49 (3)	118 (2)	118 (2)	3h
$IrCl_2(o\text{-}N_2C_6H_4NO_2)(CO)(PPh_3)_2$	2.05 (4)	1.19 (4)	1.47 (5)	115 (3)	115 (3)	3g
		"Half Doubly Bent"				
$[IrCl(N_2Ph)(PMePh_2)_3][PF_6]$	1.835 (8)	1.241 (11)	1.421 (11)	1.55.2 (7)	118.8 (8)	13
$Mo(N_2Ph)_2(TTP)$	2.060 (5)	1.133 (9)	1.448 (12)	149.1 (9)	128.6 (9)	this work

[a] PPP = $PhP(CH_2CH_2CH_2PPh_2)_2$.

plexes suggesting considerably less π interaction between the metal and adjacent nitrogen of the N_2Ph ligand.

Usually, the M–N–N–Ph linkage is planar.[3,4] It is not the case in $Mo(N_2Ph)_2(TTP)$ as reflected by the torsion angles (MoN_2,N_2C) = 73° and (N_2C,Ph_7) = 59.7°. This particular geometry seems to result from crystal packing. As shown in Figure 3, the phenyl group of the diazo ligand lies in a parallel and staggered position with respect to a tolyl group of a neighboring molecule. The distance between the two aromatic rings is 3.6 Å.

In addition the N(6)–N(7) distance of 2.928 Å reveals a weak hydrogen bond between the nitrogen atom N(6) of the diazo ligand and the phenylhydrazine of crystallization. As the NH group of the solvate molecule involved in this hydrogen bond with N(6) is disordered (occupancy factor of $^1/_2$), this hydrogen bond induces a slight disorder to N(6). Thus, a large thermal motion due to disorder affects N(6), and consequently the N(5)–N(6) bond length of 1.133 (9) Å is slightly too short. On the other hand, the thermal motion of N(5) is small so that the Mo–N(5) bond distance of 2.060 (5) Å is not affected by the slight disorder of N(6).

If one regards the singly bent aryldiazo as N_2Ph^+ and the doubly bent ligand as N_2Ph^-, the formal oxidation state of Mo is correspondingly either Mo(0) or Mo(IV). In the nitrosyl derivative $Mo(NO)_2(TTP)$, the two nitrosyl groups are in cis position with respect to the porphyrin ligand, and in view of the Mo–N(NO) distances (1.70 (1) Å), it may be described as a Mo(0) complex, $Mo^0(NO^+)_2(TTP)$, despite the nonlinearity of the Mo–N–O linkage. Ignoring possible steric effects, the complexes $Mo(N_2Ph)_2(TTP)$ and $Mo(NO)_2(TTP)$ should have the same geometry if N_2Ph^+ were present, since N_2Ph^+ and NO^+ are formally isoelectronic. The only example of six-coordinate molybdenum(IV)–porphyrin complexes is $MoCl_2(TTP)$ which exhibits two chlorines in trans configuration. Thus, considering the geometry and the Mo–N(N_2Ph) bond length, the present aryldiazo complex is formally best described as $Mo^{IV}(N_2Ph)_2(TTP)$.

Acknowledgment. G.B. wishes to thank the Centre National de la Recherche Scientifique for a 1-year fellowship (ATP Internationale No. 2.556).

Registry No. $Mo(N_2C_6H_5)_2(TTP)\cdot C_6H_5NHNH_2$, 75030-68-1; $MoCl_2(TTP)$, 64024-40-4.

Supplementary Material Available: Listings of observed and calculated structure factors (10 pages). Ordering information is given on any current masthead page.

Contribution from the Department of Chemistry,
The University of North Carolina, Chapel Hill, North Carolina 27514

Calculation of Electron-Transfer Rate Constants from the Properties of Charge-Transfer Absorption Bands. The PQ^{2+},$Fe(CN)_6^{4-}$ System

JEFF C. CURTIS, B. PATRICK SULLIVAN, and THOMAS J. MEYER*

Received February 20, 1980

The properties of the outer-sphere optical charge-transfer (CT) band in the ion pair $Fe(CN)_6^{4-}$,PQ^{2+} (where PQ^{2+} = 1,1′-Me_2-4,4′-bpy^{2+}) are used to calculate the rate constant for intermolecular electron transfer within the ion pair, $Fe(CN)_6^{4-}$,$PQ^{2+} \rightleftharpoons Fe(CN)_6^{3-}$,$PQ^+$, and from that value and an appropriate thermochemical cycle, a rate constant for the overall reaction, $PQ^{2+} + Fe(CN)_6^{4-} \rightarrow PQ^+ + Fe(CN)_6^{3-}$, can be calculated ($k_{12} = (0.2\text{–}3) \times 10^{-4}$ M^{-1} s^{-1}, I = 0.10 M, 23 °C, in water). The calculated value compares well with a value estimated with the use of self-exchange rate constants for the $PQ^{2+/+}$ and $Fe(CN)_6^{3-/4-}$ couples and the Marcus cross-reaction equation ($k_{12} = 10^{-3}$ M^{-1} s^{-1}). The results obtained suggest that for a variety of CT-type transitions it may be possible to obtain detailed information about the innate electron-transfer characteristics of the redox sites involved from a straightforward analysis of the absorption band.

The observation of optical electron transfer between electronically weakly coupled redox sites provides, in principle, a means for exploring in detail the relationships between spectral transition energies, thermodynamics, and electron-transfer processes. Especially well documented are the low-energy transitions which appear in mixed-valence dimers or

0020-1669/80/1319-3833$01.00/0

association complexes

$$(bpy)_2ClRu^{II}N\bigcirc NRu^{III}Cl(bpy)_2^{3+} \xrightarrow{h\nu} (bpy)_2ClRu^{III}N\bigcirc NRu^{II}Cl(bpy)_2^{3+} \quad (1)^1$$

$$Fe^{II}(CN)_6^{4-}, (NH_3)_5Ru^{III}(py)^{3+} \xrightarrow{h\nu} Fe^{III}(CN)_6^{3-}, (NH_3)_5Ru^{II}(py)^{2+} \quad (2)^2$$

(bpy = 2,2′-bipyridine; py = pyridine).

These mixed-valence or metal–metal charge-transfer (MMCT) transitions have been termed "intervalence transfer" (IT) by Hush,[3] who has shown that their properties should be related quantitatively to the corresponding thermal electron-transfer processes[4]

$$(bpy)_2ClRu^{II}N\bigcirc NRu^{III}Cl(bpy)_2^{3+} \xrightarrow{k_{et}} (bpy)_2ClRu^{III}N\bigcirc NRu^{II}Cl(bpy)_2^{3+} \quad (3)$$

$$Fe^{II}(CN)_6^{4-}, (NH_3)Ru^{III}(py)^{3+} \xrightarrow{k_{et}} Fe^{III}(CN)_6^{3-}, (NH_3)_5Ru^{II}(py)^{2+} \quad (4)$$

In order to test the relationship between optical and thermal electron transfer suggested by theory, we have turned to spectral and redox potential measurements on the ion pair PQ^{2+},$Fe(CN)_6^{4-}$, where PQ^{2+} (paraquat) is the dicationic

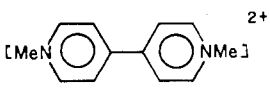

paraquat

organic acceptor 1,1′-dimethyl-4,4′-bipyridinium ion. The ion pair exhibits a relatively low-energy absorption band readily visible to the eye as a deep purple in sufficiently concentrated solutions of the two ions, as reported initially by Nakahara and Wang[5] and by Toma.[6] The origin of the band is undoubtedly a charge-transfer transition between adjacent redox sites analogous to the IT transitions in eq 1 and 2.

The approach taken will be to use the properties of the absorption band to calculate both the exponential and preexponential terms for the related thermal electron-transfer process between the two ions in the ion pair. By introducing the thermodynamic properties associated with ion-pair formation, it is possible to test the spectroscopically derived information about thermal electron transfer with experimental data. The experimental data of relevance are the outer-sphere electron-transfer self-exchange rate constants for the couples $Fe(CN)_6^{3-/4-}$ and $PQ^{2+/+}$.

Experimental Section

Materials. $K_4Fe(CN)_6 \cdot 3H_2O$ was purchased from Baker & Adamson and recrystallized once from water. 1,1′-Dimethyl-4,4′-bipyridinium (paraquat or methylviologen) was purchased from Aldrich as the dichloride salt and used without further purification. Deionized water was distilled once from $KMnO_4$ and used without further purification.

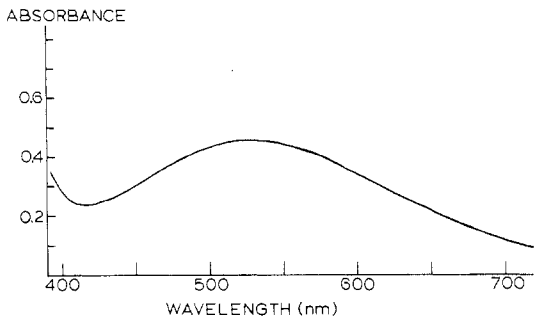

Figure 1. Charge-transfer band for the ion pair $Fe^{II}(CN)_6^{4-}$,PQ^{2+} in water at 23 ± 2 °C (1-mm path length; $[Fe^{II}(CN)_6^{4-}] = [PQ^{2+}] = 0.10$ M; in 0.09 M $Na(CF_3CO_2)$ and 0.01 M KHP pH 5 buffer).

Measurements. Spectra were recorded on a Cary 17 spectrophotometer. Temperature-dependent data were obtained with use of a Forma Scientific Jr. constant-temperature bath and a circulating cell block in the spectrophotometer cell holder.

Electrochemical data were obtained by cyclic voltammetry using a locally designed waveform generator, a PAR 174 potentiostat, and a Hewlett-Packard 7004B XY recorder. A freshly polished gold-disk electrode was used in each experiment. Temperature-dependence data were obtained by immersing cells containing solutions of $Fe(CN)_6^{4-}$ or PQ^{2+} (1 mM) in a constant-temperature bath. Cyclic voltammograms were then recorded at a given temperature vs. a thermally isolated, room-temperature, saturated calomel electrode (SCE). The $E_{1/2}$ values for each cell were taken as the average of the oxidative and reductive peak potentials. The values used were average values for several scans obtained at scan rates of 200, 100, 50, and 20 mV/s. Ionic strength was maintained at 0.1 M by a 0.09 M sodium trifluoroacetate electrolyte and a 0.01 M, pH 5 potassium biphthalate buffer system.

Results and Discussion

Analysis of the PQ^{2+},$Fe(CN)_6^{4-}$ Charge-Transfer Band. The outer-sphere, intervalence charge-transfer (CT) band for the $Fe(CN)_6^{4-}$,PQ^{2+} ion pair is shown in Figure 1. The band is approximately Gaussian in shape and has a maximum at 530 ± 2 nm ((18.87 ± 0.07) × 10^3 cm^{-1}), which shifts slightly to higher energy in highly concentrated solutions containing both ions. The slight shift no doubt reflects the formation of higher ion aggregates.[5] $Fe(CN)_6^{4-}$ and PQ^{2+} do not absorb significantly by themselves in this spectral region.

The bandwidth at half-maximum is 6800 ± 300 cm^{-1}. The band is broader by a factor of 1.5 than the value predicted by Hush for IT bands using the relation

$$\Delta\nu_{1/2}(\text{theor}) = [2.31 \times 10^3(E_{op} - \Delta E)]^{1/2} = 4630 \text{ cm}^{-1} \quad (5)$$

where E_{op} and ΔE are measured in cm^{-1}. E_{op} is the energy of the optical transition and ΔE is the internal energy difference between the two thermally equilibrated redox isomeric states

$$PQ^{2+},Fe(CN)_6^{4-} \xrightarrow{\Delta E} PQ^{+},Fe(CN)_6^{3-} \quad (6)$$

Equation 5 is expected to be valid only for certain limiting conditions: high-temperature classical limit, equal vibrational force constants for the normal vibrational modes in each redox isomeric state, harmonic oscillator vibrations, and the applicability of the Born–Oppenheimer approximation.[3,7] In practice, bandwidths broader than those predicted by eq 4 are

(1) Callahan, R. W.; Keene, F. R.; Meyer, T. J.; Salmon, D. J. *J. Am. Chem. Soc.* **1977**, *99*, 1064. Meyer, T. J. *Acc. Chem. Res.* **1978**, *11*, 94; *Ann. N.Y. Acad. Sci.* **1978**, *313*, 496. Taube, H. *Ibid.* **1978**, *313*, 481.
(2) (a) Curtis, J. C.; Meyer, T. J. *J. Am. Chem. Soc.* **1978**, *100*, 6284. (b) Toma, H. J. *J. Chem. Soc., Dalton Trans.* **1980**, *3*, 471.
(3) Hush, N. S. *Prog. Inorg. Chem.* **1961**, *8*, 391.
(4) (a) Meyer, T. J. *Chem. Phys. Lett.* **1979**, *64*, 417. (b) Curtis, J. C.; Meyer, T. J., manuscript in preparation.
(5) Nakahara, A.; Wang, J. H. *J. Phys. Chem.* **1963**, *67*, 496.
(6) Toma, H. E. *Can. J. Chem.* **1979**, *57*, 2079.
(7) Meyer, T. J. In "Mixed-Valence Compounds in Chemistry, Physics and Biology"; Brown, D. B., Ed.; Reidel Publishing Co.: Dordrecht, Holland, in press.

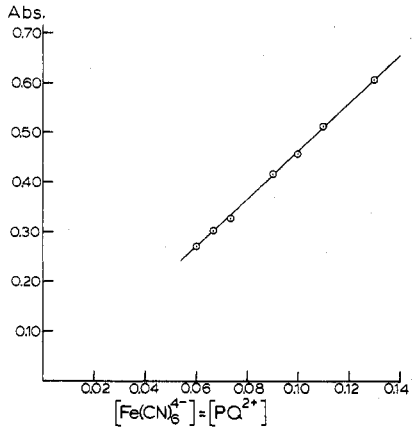

Figure 2. Beer's law plot for the ion pair $Fe^{II}(CN)_6^{4-}$,PQ^{2+} in 0.09 M $Na(CF_3CO_2)$ and 0.01 M KHP pH 5 buffer at 23 ± 2 °C (1-mm path length).

Table I. Ion-Pair Formation as a Function of Reactant Concentration[a]

$[Fe^{II}(CN)_6^{4-}] = [PQ^{2+}]$, 10^{-3} M (initial)	absorbance[b]	$[Fe^{II}(CN)_6^{4-},PQ^{2+}]$,[c] 10^{-4} M	K_{IP},[d] M^{-1}
0.7	0.045	0.89	238
0.9	0.063	1.26	210
1.0	0.085	1.70	247
1.4	0.143	2.86	230
1.8	0.187	3.74	184
2.0	0.244	4.88	213
2.5	0.332	6.64	197

[a] Experiments were performed at 23 ± 2 °C in 0.09 M NaTFA and 0.01 M KHP buffer; pH 4. [b] At 530 nm; 10-cm path length. [c] Using $\epsilon = 50 \pm 5$ cm^{-1} M^{-1}. [d] $K_{IP} = \{[PQ^{2+}]/[Fe^{II}(CN_6^{4-},PQ^{2+}] - 2[PQ^{2+}] + [Fe^{II}(CN)_6^{4-},PQ^{2+}]\}^{-1}$ where $[PQ^{2+}]$ is the initial concentration of paraquat.

commonly found for IT bands in mixed-valence dimers and ion pairs.[1,2]

The extinction coefficient for the CT band was obtained from a simple Beer's law plot in a concentration region where ion pairing was complete. Complete ion pairing is shown by the linearity in the absorbance vs. concentration plot (Figure 2). The slope of the line leads straightforwardly to an extinction coefficient of 50 ± 2 M^{-1} cm^{-1}. This value is somewhat less than the value of 73 M^{-1} cm^{-1} obtained by Nakahara and Wang using a more complicated technique involving a large excess of paraquat and a resultant mixture of 1:1 and 2:1 ion pairs.[5]

Knowing the extinction coefficient of the ion pair for the CT band allows the ion-pair association constant to be determined spectrally. The extent of ion-pair formation was measured as a function of reactant concentrations (equimolar) in a concentration region where ion pairing is significantly *less* than complete. The absorbance at 530 nm was monitored at various concentrations between 7.0×10^{-4} and 2.5×10^{-3} M in each ion. The results, which are summarized in Table I, lead to an average value of 220 ± 30 M^{-1} at 23 ± 2 °C and $I = 0.1$ M.

An alternate method for determining both the association constant, K^A_{12}, and the extinction coefficient, ϵ_{IP}, relies on the use of the data from Table I and eq 7, which is a rearranged

$$\frac{[A]_0}{OD} = \frac{1}{K^A_{12}}\frac{1}{[D]_0} + \frac{[A]_0}{[D]_0\epsilon_{IP}} + \frac{1}{\epsilon_{IP}} - \frac{[AD]}{\epsilon_{IP}[D]_0} \quad (7)$$

form of the equilibrium constant expression based on the assumption that $OD = \epsilon_{IP}[AD]$ (OD is absorbance or optical density, [AD] is the ion-pair or association complex concentration).[8] In eq 7, $[A]_0$ and $[D]_0$ are the initial concentrations of acceptor (PQ^{2+}) and donor ($Fe(CN)_6^{4-}$), respectively. Under the experimental conditions used to obtain the data in Table I, $[A]_0 = [D]_0$ and $[AD] \ll [A]_0$. Given the latter conditions, the last term in eq 7 can be neglected, and by simplification and rearrangement, eq 8 is obtained. The

$$1/[A]_0 = (K^A_{12}\epsilon_{IP})[A]_0/OD - 2K^A_{12} \quad (8)$$

graphical representation of eq 8 using the data from Table I is shown in Figure 3. The graphical analysis (correlation coefficient $r = 0.980$) yields $\epsilon_{IP} = 47 \pm 3$ and $K^A_{12} = 256 \pm 25$, which are in reasonable agreement with the method discussed above.

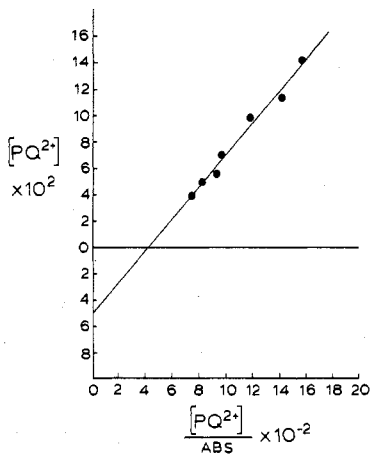

Figure 3. Alternate determination of ϵ_{IP} and K^A_{12} for the conditions $[PQ^{2+}] = [Fe^{II}(CN)_6^{4-}]$ and $[PQ^{2+},Fe(CN)_6^{4-}] \ll [PQ^{2+}]$. Data and conditions are cited in Table I.

Scheme I

$$Fe^{II}(CN)_6^{4-} + PQ^{2+} \xrightarrow{\Delta G^{\circ\prime}_{12}} Fe^{III}(CN)_6^{3-} + PQ^{+}$$
$$\Delta G_1^A \downarrow \qquad\qquad \Delta G_2^A \uparrow$$
$$[Fe^{II}(CN)_6^{4-}, PQ^{2+}] \xrightarrow{\Delta G^{\circ\prime}_{IP}} [Fe^{III}(CN)_6^{3-}, PQ^{+}]$$

These values of the extinction coefficient and association constant differ somewhat from those reported by Toma, which are 150–200 M^{-1} cm^{-1} and 30–40 M^{-1}, respectively.[6] Since the method used in this work involves a straightforward, stepwise determination of the two quantities involved, we feel that they are probably more accurate than values obtained via iterative methods where the two quantities are determined simultaneously as in the work of Wang and of Toma. In our experiments the ionic strength of the medium was held at 0.1 M with the use of 0.09 M sodium trifluoroacetate and a 0.01 M potassium biphthalate buffer which maintained the pH at 5.

Thermodynamic Quantities for Electron Transfer within the Ion Pair. Our goal here is to use the properties of the CT band for the ion pair to calculate an electron-transfer rate constant for the thermodynamically nonspontaneous electron-transfer reaction within the ion pair $PQ^{2+},Fe^{II}(CN)_6^{4-} \rightarrow PQ^{+},Fe^{III}(CN)_6^{3-}$. The optically derived result will then be compared to a calculated result for the outer-sphere reaction $PQ^{2+} + Fe(CN)_6^{4-} \rightarrow PQ^{+} + Fe(CN)_6^{3-}$, where the calculation is based on self-exchange rate constants for the $Fe(CN)_6^{3-/4-}$ and $PQ^{2+/+}$ couples. The thermodynamics of the two different processes are interrelated by the thermochemical cycle in Scheme I. In order to connect them, it is necessary to evaluate the various thermodynamic quantities in the cycle.

(8) Foster, R. "Organic Charge Transfer Complexes"; Academic Press: New York, 1970.

Table II. Temperature Dependence of $\Delta E_{1/2}$ for the Overall Reaction $Fe^{II}(CN)_6^{4-} + PQ^{2+} \rightarrow Fe^{III}(CN)_6^{3-} + PQ^{2+}$ [a]

T, K	$E_{1/2}$ $(Fe(CN)_6^{3-/4-})$, V	$E_{1/2}$ $(PQ^{2+/+})$, V[b]	$-\Delta E_{1/2}$, V
273.91	0.203 ± 0.005	−0.681 ± 0.005	0.884 ± 0.015
273.9	0.203	−0.687	0.890
275.5	0.189	−0.682	0.871
281.0	0.190	−0.682	0.872
281.3	0.191	−0.684	0.875
284.2	0.184	−0.681	0.865
284.3	0.194	−0.684	0.878
287.1	0.187	−0.683	0.869
291.9	0.170	−0.689	0.859
301.1	0.165	−0.690	0.855
305.7	0.168	−0.690	0.859
310.8	0.156	−0.691	0.847

[a] Potentials were obtained on a polished gold-disk electrode in a medium of 0.09 M $Na(CF_3CO_2)$ and 0.01 M pH 5 KHP buffer and are vs. a SCE reference electrode at room temperature. [b] PQ^{2+} cell was purged of oxygen by nitrogen bubbling.

From the cycle, the free-energy change associated with electron transfer within the ion pair is given by eq 9. From

$$\Delta G^{\circ\prime}_{IP} = \Delta G^{\circ\prime}_{12} - \Delta G^{A}_{1} + \Delta G^{A}_{2} \quad (9)$$

the difference in the electrochemically determined $E_{1/2}$ values for the $Fe(CN)_6^{3-/4-}$ and $PQ^{2+/+}$ couples, $\Delta G^{\circ\prime}_{12}(23\ ^\circ C) = -nF(\Delta E^{\circ\prime}) = 19.8 \pm 0.2$ kcal/mol, since $\Delta E^{\circ\prime}(23\ ^\circ C) = +0.858 \pm 0.008$ V (Table II).

The free energy of association between PQ^{2+} and $Fe(CN)_6^{4-}$ at 23 °C is obtained readily from the association constant as $\Delta G^{A}_{1} = -RT \ln K^{A}_{12} = -3.1 \pm 0.1$ kcal/mol ($K^{A}_{12} = 220 \pm 30\ M^{-1}$). ΔG^{A}_{2} cannot be evaluated directly since an experimental value for the associated equilibrium constant is not available. However, a theoretical estimate can be made with use of the Eigen–Fuoss equation[9] (eq 10), where Z_1 and Z_2

$$\Delta G^{A} = \frac{Z_1 Z_2 e^2}{D_s d}\left(\frac{1}{1 + \kappa d}\right) - RT \ln \frac{4\pi N_0 d^3}{3000} \quad (10)$$

are the charges on the reactants, $e^2 = 3.318 \times 10^{-3}$ cal cm/mol, D_s is the dielectric constant (78.5 for H_2O at 23 °C), d is the hard-sphere interreactant contact distance measured in cm, κ is the Debye inverse length ($0.329I^{1/2}/10^{-8}$ cm^{-1} for H_2O at 23 °C), and N_0 is Avogadro's number.

However, we reason that a more accurate estimate can be obtained in the following way. We have an experimental value for ΔG^{A}_{1} and can use eq 10 to obtain a calculated value. With the assumption that the form of eq 10 is correct with regard to the dependence of the factor $Z_1Z_2e^2/d$, the ratio of experimental to calculated values provides a general "correction factor" for the type of association reaction dealt with here. A more accurate estimate should be obtainable from eq 11.

$$\Delta G^{A}_{2} = [\Delta G^{A}_{2}(\text{Eigen–Fuoss})]\frac{\Delta G^{A}_{1}(\text{exptl})}{\Delta G^{A}_{1}(\text{Eigen–Fuoss})} \quad (11)$$

For $Fe^{II}(CN)_6^{4-}$ the close-contact "hard-sphere" radius is 4.6×10^{-8} cm as calculated from crystallographic data and the known nitrogen van der Waals radius;[10] for PQ^{2+} an upper boundary for the effective radius is 3.5×10^{-8} cm as calculated from the volume-increment approach of Bondi.[11a,b] A lower boundary of 1.7×10^{-8} cm, which would be appropriate if the π system of PQ^{2+} is in close contact with $Fe(CN)_6^{4-}$, is the van der Waals radius of the aromatic π system. There is crystallographic evidence for this type of close contact between the aromatic PQ^{2+} nitrogen atom and metal-coordinated chloride ligands in the system $[PQ]CoCl_4$.[11c] Thus d must be within the range $(8.1–6.3) \times 10^{-8}$ cm, and ΔG^{A}_{1}(Eigen–Fuoss) is in the range −2.4 to −3.0 kcal/mol, which is in reasonably good agreement with the experimental value (−3.2 kcal/mol). The correction factor in eq 12 is then between 1.3 and 1.1, and from eq 11 and 12, ΔG^{A}_{2} lies in the range −1.3 to −1.0 kcal/mol. Using the values obtained for $\Delta G^{\circ\prime}_{12}$, ΔG^{A}_{1}, and ΔG^{A}_{2} in eq 9 gives for the free-energy change on electron transfer within the ion pair $\Delta G^{\circ\prime}_{IP} = 21.7 \pm 0.4$ kcal/mol. By comparing $\Delta G^{\circ\prime}_{12}$ for the overall reaction with $\Delta G^{\circ\prime}_{IP}$, we find that the redox asymmetry for electron transfer inside the ion pair is increased by 1.9 kcal/mol (0.08 V) over that inherent in the redox asymmetry between the separated couples.

An analogous cycle can be used to obtain $\Delta S^{\circ\prime}_{IP}$, the entropy change associated with electron transfer inside the ion pair. Note Scheme II.

Of the thermodynamic quantities in Scheme II, $\Delta S^{\circ\prime}_{12}$ can be obtained from the temperature dependence of the difference

Scheme II

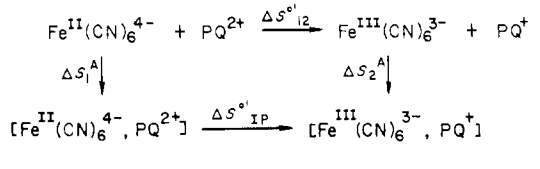

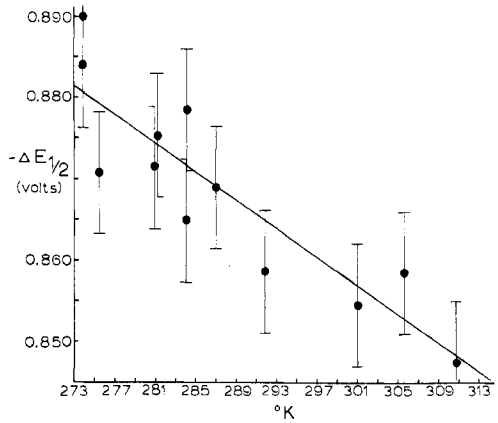

Figure 4. Temperature dependence of $\Delta E_{1/2}$ for the overall reaction $Fe^{II}(CN)_6^{4-} + PQ^{2+} \rightarrow Fe^{III}(CN)_6^{3-} + PQ^{+}$.

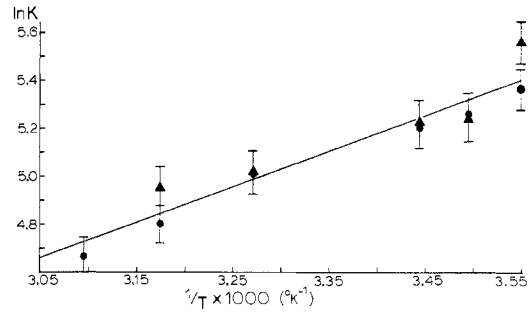

Figure 5. Temperature dependence of the ion-pair formation constant K^{A}_{12}. The solid dots refer to both $[Fe(CN)_6^{4-}]$ and $[PQ^{2+}] = 0.0025$ M, and for the triangles the concentration of each reagent is 0.0015 M (in 0.09 M $Na(CF_3CO_2)$ and 0.01 M KHP pH 5 buffer; 10-cm path length).

(9) Fuoss, R. M. *J. Am. Chem. Soc.* **1958**, *80*, 5059.
(10) (a) Sharpe, A. G. "The Chemistry of Cyano Complexes of Transition Metals"; Academic Press: New York, 1976; p 104. (b) "Handbook of Chemistry and Physics", 53rd ed.; CRC Press: Cleveland, Ohio, 1973; p D146.
(11) (a) Bondi, A. *J. Phys. Chem.* **1964**, *68*, 441. (b) Edward, J. T. *J. Chem. Educ.* **1970**, *17*, 261. (c) Prout, C. K.; Murray-Rust, P. *J. Chem. Soc. A* **1979**, 1520.

in $E_{1/2}$ values for the two couples (Table II). The $\Delta E_{1/2}$ data $[(E_{1/2}(PQ^{2+/+}) - E_{1/2}[Fe(CN)_6^{3-/4-})]$ are shown plotted in Figure 4 against temperature. From the slope of the least-squares line in Figure 4, $\Delta S^{\circ\prime}_{12} = 8.7 \times 10^{-4}$ V/K or $+20 \pm 5$ eu. ΔS^{A}_{1}, the entropy of association for the reactants, was determined spectrophotometrically from the temperature dependence of the ion-pair formation constant. The intercept of the plot shown in Figure 5 gives $\Delta S^{A}_{1} = +0.3 \pm 5$ eu.

To estimate ΔS^{A}_{2}, we must again have recourse to theory. Two treatments are available for predicting entropies of association. The first is a simple extension of the Eigen–Fuoss model and has been outlined recently by Brown and Sutin.[12] The second is based on a collisional treatment and was originally developed by North.[13] This approach has been applied to electron-transfer reactions by both Marcus[14] and Sutin.[12] For the case considered here, the collisional treatment gives far better agreement between theory and experiment when applied to ΔS^{A}_{1}.

The collisionally derived entropy of association[12,14] is given by eq 12–14, where μ is the reduced mass in grams for the

$$\Delta S^{A} = \Delta S_{trans} - \frac{\partial W_r}{\partial T} \tag{12}$$

$$\Delta S_{trans} = R \ln [(Nd^2/1000)(8\pi h^2/\mu k_b T)^{1/2}] - R/2 \tag{13}$$

$$\frac{\partial W_r}{\partial T} = \left(\frac{-Z_1 Z_2 e^2}{D_s d T}\right)\frac{2\theta + \theta\kappa d + \kappa d}{2(1 + \kappa d)^2} \tag{14}$$

ion pair, k_b is Boltzmann's constant, h is Planck's constant, θ is the quantity $-\partial \ln D_s/\partial \ln T$ (1.368 for H_2O at 25 °C),[12] and all other symbols are as previously defined. The ΔS_{trans} term arises because of the loss of a translational degree of freedom upon formation of the association complex,[13] and the $\partial W_r/\partial T$ term results from the temperature dependence of the electrostatic work term[14]

$$W_r = Z_1 Z_2 e^2/D_s d(1 + \kappa d) \tag{15}$$

For these calculations we will use $d = 7.2 \times 10^{-8}$ cm, which is the simple average of the two extremes discussed previously. Since d is essentially the same for the redox configurations both before and after electron transfer, PQ^{2+},$Fe(CN)_6^{4-}$ and PQ^{+},$Fe(CN)_6^{3-}$, eq 13 predicts that ΔS_{trans} will be the same for both ΔS^{A}_{1} and ΔS^{A}_{2} and the calculated value is $\Delta S_{trans} = -7.4$ eu. The entropic work term will of course be different for the two ion pairs because of the different charge types involved. The calculated values are $\partial W_{r1}/\partial T = +11.7$ eu and $\partial W_{r2}/\partial T = +4.4$ eu. Theoretically, calculated values for the two entropic changes are $\Delta S^{A}_{1} = +4.3$ eu (ΔS^{A}_{1}(exptl) = +0.3 eu) and $\Delta S^{A}_{2} = +3.0$ eu. Once again, a best estimate for ΔS^{A}_{2} is probably obtainable by correcting the calculated value by the ratio of the observed to predicted values for ΔS^{A}_{1}. Thus $\Delta S^{A}_{2} = -3.0(0.3/4.3) = -0.2 \pm 5$ eu. From the entropic cycle in Scheme II it follows that $\Delta S^{\circ\prime}_{IP} = \Delta S^{\circ}_{12} - \Delta S^{A}_{1} + \Delta S^{A}_{2} = 20 - 0.3 - 0.2 \cong +19.5 \pm 5$ eu. This calculation suggests that the entropic change accompanying electron transfer within the ion pair is not significantly different from that for the isolated reactants and products.

In order to complete the analysis of the thermodynamic terms which relate to two types of electron-transfer processes, the heat change associated with electron transfer within the ion pair is given by $\Delta H^{\circ\prime}_{IP} = \Delta G^{\circ\prime}_{IP} + T\Delta S^{\circ\prime}_{IP}$. In the absence of pressure–volume work, $\Delta H = \Delta E$, and so the internal energy change associated with electron transfer within the ion pair is given by $\Delta H^{\circ\prime}_{IP} = \Delta E = 27.3 \pm 1.0$ kcal/mol.

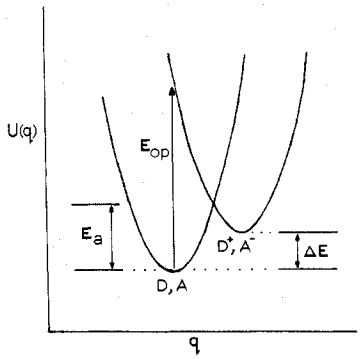

Figure 6. Potential energy diagram for the reactants (D,A) and products (D^+,A^-) for the case where $\Delta E > 0$.

Basis for the Comparison between Spectral and Kinetic Data. The theoretical work of Hush, which is semiclassical in nature, and more recent quantum mechanically based theory provide the means for comparing spectral and kinetics data on electron-transfer processes. In Figure 6 is shown a potential energy diagram which is relevant to the point of comparing optical and thermal electron transfers in an unsymmetrical redox system where the Born–Oppenheimer separation is appropriate. The figure can be viewed as being a plot of the potential energy $U(q)$ vs. displacement coordinate q for a single normal mode of the system which responds to the change in electron distribution in the two different electronic states D,A and D^+,A^-. Alternatively, it can be viewed as the $U(q)$ vs. q distribution along a plane drawn through the actual multidimensional potential surface. The multidimensional surface includes contributions from all of the relevant solvent and intramolecular vibrations.

For the case where q is a generalized coordinate, in the high-temperature, classical limit, the energy quantities shown on the diagram representing optical (E_{op}) and thermal (E_a) electron transfers for the process D,A → D^+,A^- are related by[3,7] eq 16. There are both solvent (χ_0) and molecular (χ_i)

$$E_a = \frac{E_{op} - \Delta E}{4}\left(1 + \frac{\Delta E}{E_{op} - \Delta E}\right)^2 = \frac{E_{op}^2}{4(E_{op} - \Delta E)} \tag{16}$$

vibrational contributions to E_{op}, and the relationship between E_{op} and ΔE is given by eq 17. Equation 17 is valid under the

$$E_{op} = \chi_0 + \chi_i + \Delta E \tag{17}$$

same limiting conditions as those for eq 5: high-temperature limit, weak electronic coupling, equal force constants in the two electronic states, and the applicability of the Born–Oppenheimer approximation.

When the problem is treated quantum mechanically,[15] an expression is derivable for the thermal rate constant for electron transfer which gives both exponential and preexponential terms (eq 18), where the preexponential term, ν_{et}, is

$$k_{et} = \nu_{et} \exp(-E_a/RT) \tag{18}$$

given by eq 19 and E_a is given by eq 16 if the limiting con-

(12) Brown. G. M.; Sutin, N. *J. Chem. Soc.* **1979**, *101*, 883.
(13) North, A. M. "The Collision Theory of Reactions in Liquids"; Methuen: London, 1964.
(14) Waisman, E.; Worry, G.; Marcus, R. A. *J. Electroanal. Chem. Interfacial Electrochem.* **1977**, *82*, 9.
(15) (a) Duke, C. B. "Proceedings of the 1977 Conference on Tunneling in Biological Systems", Chance, Britton, Ed. (b) Kestner, N. R.; Logan, J.; Jortner, J. *J. Phys. Chem.* **1974**, *78*, 2148. (c) Hopfield, J. J. *Proc. Natl. Acad. Sci. U.S.A.* **1974**, *71*, 3640. (d) Chien, J. C. W. *J. Phys. Chem.* **1978**, *82*, 2158.

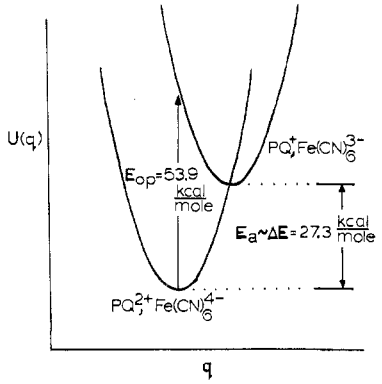

Figure 7. Potential energy diagram for the oxidation-state distributions of $PQ^{2+},Fe^{II}(CN)_6^{4-}$ and $PQ^+,Fe^{III}(CN)_6^{3-}$.

$$\nu_{et} = 2\pi \frac{V_{ab}^2}{\hbar}\left(\frac{\pi}{kT(E_{op} - \Delta E)}\right)^{1/2} \quad (19)$$

ditions mentioned above are applicable. It should be noted that eq 19 has been derived by several authors. In some of the treatments given the final form differs slightly; e.g., the derivation of Hopfield leads to the same expression but without the initial factor of 2π.[15c] In eq 19, V_{ab} is the electron-exchange matrix element, which can be estimated from the integrated intensity of the CT band.

The procedure that we will follow for comparing outer-sphere rate constant data with the properties of the optical transition is as follows. For the net reaction (eq 20), the

$$PQ^{2+} + Fe(CN)_6^{4-} \rightarrow PQ^+ + Fe(CN)_6^{3-} \quad (20)$$

mechanism of electron transfer involves an initial association followed by electron transfer within the ion pair as shown in eq 21 and 22. The thermal rate constant for the reaction is

$$PQ^{2+} + Fe(CN)_6^{4-} \overset{K^A_1}{\rightleftharpoons} PQ^{2+},Fe(CN)_6^{4-} \quad (21)$$

$$PQ^{2+},Fe(CN)_6^{4-} \xrightarrow{k_{et}} PQ^+,Fe(CN)_6^{3-} \quad (22)$$

given by eq 23 where K^A_{12} is known from experiment and k_{et}

$$k_{12} = K^A_{12}k_{et} \quad (23)$$

can be calculated from the properties of the CT absorption band.[16]

The electron-transfer rate for eq 20 cannot be measured because the reaction is nonspontaneous by a considerable extent. However, a reasonable comparison with kinetic data can still be made on the basis of the Marcus cross-reaction equation[17] (eq 24), where k_{11} and W_{11} are, for example, the

$$k_{12} = (k_{11}k_{22}K_{12}f_{12})^{1/2} \exp(W_{11} + W_{22} - W_{12} - W_{21})/2RT \quad (24)$$

$$\ln f_{12} = (\ln K_{12})^2/[4 \ln (k_{11}k_{22}/Z^2)]$$

self-exchange rate constant and electrostatic work terms for one of the redox couples in the net reaction, K_{12} is the equilibrium constant for the overall reaction, W_{12} and W_{21} are the electrostatic work terms associated with the two ion-pair steps in Scheme I, and $Z = 10^{11}$ is taken to be the bimolecular collision frequency between two uncharged reactants at unit concentration.

(16) Sullivan, B. P.; Meyer, J. T. *Inorg. Chem.*, in press. Powers, M.; Meyer, T. J. *J. Am. Chem. Soc.*, in press.
(17) Haim, A.; Sutin, N. *Inorg. Chem.* **1976**, *15*, 476.

Comparison between the Spectral and Kinetics Data. From the analysis given in the previous section, the desired comparison follows straightforwardly. The thermal activation barrier to electron transfer is given by eq 16 in terms of E_{op} and ΔE, and using the values obtained from the CT band and temperature dependent redox potential measurements, we obtain eq 25.

$$E_a = \frac{E_{op}^2}{4(E_{op} - \Delta E)} = \frac{(53.9)^2}{4(53.9 - 27.3)} = 27.3 \text{ kcal/mol} \quad (25)$$

With ΔE and E_a values in hand, it is possible to illustrate the energy relationships involved for the $PQ^{2+},Fe(CN)_6^{4-}$ ion pair, and they are shown on the potential energy diagram in Figure 7. It is a striking result since it shows that the reaction under consideration is at or near the enthalpic analogue of the Marcus "abnormal" free-energy region and that the reverse reaction, eq 26, is close to being a relaxation process for an outer-sphere CT excited state.[18-20]

$$PQ^+,Fe(CN)_6^{3-} \rightarrow PQ^{2+},Fe(CN)_6^{4-} \quad (26)$$

The preexponential term in eq 18 can be calculated by using ΔE from the temperature-dependent redox potential measurements and two properties of the CT band, the band energy and its integrated intensity. The integrated band intensity is related to the electron-exchange matrix element through α

$$V_{ab} = E_{op}\alpha \quad (27)$$

where α^2, which is a measure of the extent of delocalization of the excess electron from the donor to the acceptor site, is given by[3]

$$\alpha^2 = 4.24 \times 10^{-20}\epsilon_{max}\Delta\nu_{1/2}/E_{op}d^2 \quad (28)$$

In eq 28, d, the interreactant distance, is in cm, ϵ_{max} is the molar extinction coefficient at λ_{max}, and $\Delta\nu_{1/2}$ is the bandwidth at half-height and is expressed, as is E_{op}, in molecular energy units. From the CT band we calculate that $\alpha^2 = (1.2\text{–}2.0) \times 10^{-4}$ and that $\nu_{et} = (6.5\text{–}10.8) \times 10^{13}$ s^{-1} by using the limiting values of 8.1×10^{-8} and 6.3×10^{-8} cm for d. The value for α^2 is typical of values found for outer-sphere complexes and electronically weakly coupled ligand-bridged dimers.[1,2,16]

We now have available an experimental value for K^A_{12} (220 ± 30) and calculated values for ν_{et} and E_a using eq 16 and 19 and the properties of the CT band. It follows from eq 18 that $k_{et} = (7\text{–}12) \times 10^{-7}$ s^{-1} and from eq 23 that $k_{12} = (2\text{–}3) \times 10^{-4}$ M^{-1} s^{-1} (I = 0.10 M; T = 23 °C).

In order to estimate the same rate constant from self-exchange rate data and redox potential values, we turn to eq 24. The ferrocyanide–ferricyanide self-exchange rate constant is 1.9×10^4 M^{-1} s^{-1} under reaction conditions similar to the ones used here,[17,21] and the $PQ^{2+/+}$ self-exchange rate constant has been estimated as 8×10^6 M^{-1} s^{-1}.[19] From the redox potential measurements, K_{12} is 1.1×10^{-16} and f_{12} is 1.5×10^{-6}, which when inserted into eq 24 give $k_{12} \cong 10^{-3}$ M^{-1} s^{-1}.

In actual fact, eq 19 for the frequency factor may be inappropriate for our case.[22] Equation 19 was derived for the nonadiabatic case where electronic coupling is weak and the rate of oscillation of the odd electron between redox sites in the intersection region between surfaces is slow relative to vibrational time scales. For the ion pair, V_{ab} is on the order 200 cm^{-1} and the calculated value for ν_{et} is rapid on the vi-

(18) Carapellucci, D. A.; Mauzerall, D. *Ann. N.Y. Acad. Sci.* **1975**, *244*, 214.
(19) Bock, C. R.; Connor, J. A.; Gutierrez, A. R.; Meyer, T. J.; Whitten, D. G.; Sullivan, B. P.; Nagle, J. K. *Chem. Phys. Lett.* **1979**, *61*, 522.
(20) Nagle, J. K.; Dressick, W. J.; Meyer, T. J. *J. Am. Chem. Soc.* **1979**, *101*, 3993.
(21) Shporer, M.; Ron, G.; Lowenstein, A.; Navon, G. *Inorg. Chem.* **1965**, *4*, 361.
(22) Brunschwig, B. S.; Logan, J.; Newton, M. D.; Sutin, N., private communication.

brational time scale. A possibly more appropriate choice for the frequency factor in the adiabatic limit is k_bT/h, which lowers the optically predicted rate constant by 1 order of magnitude giving $k_{12} \geq 2 \times 10^{-5}$ M^{-1} s^{-1}.

In any case, given the estimates needed in calculating the two values for k_{12}, the agreement obtained is remarkable. Although further tests of this kind are essential, of the examples where CT transitions have been used to estimate thermal electron-transfer rate constants, the agreement obtained[4] and the prospects for future experiments of the same kind in a variety of systems are very encouraging. In any given system, a detailed theoretical understanding of the full solvent and molecular contributions to E_{op} may be difficult. However, in principle, these details are contained intrinsically in the properties of the optical transition. As long as the optical and thermal processes are related, what can be measured optically is also known for the thermal process. The possibility clearly exists that for a variety of CT-type transitions the properties of the optical absorption bands contain detailed information about the innate electron-transfer characteristics of the redox sites involved and that this information may be obtainable by a relatively simple deconvolution of CT absorption bands.

Acknowledgments are made to the Army Research Office under Grant No. DAAG29-79-C-0044 and to the National Science Foundation under Grant No. CHE77-03423 for support of this research. The authors also thank Dr. Norman Sutin for a helpful discussion and for having kindly provided a preprint of ref 22.

Registry No. $Fe(CN)_6^{3-}$, 13408-62-3; $Fe(CN)_6^{4-}$, 13408-63-4; PQ^{2+}, 4685-14-7; PQ^{+}, 25239-55-8.

Notes

Contribution from the Istituto di Chimica Generale ed Inorganica, Università di Firenze, Laboratorio CNR, Florence, Italy

ESR Spectra of Low-Symmetry High-Spin Cobalt(II) Complexes. 7.[1] Trigonal-Bipyramidal Pentakis(picoline *N*-oxide)cobalt(II) Perchlorate

A. Bencini, C. Benelli, D. Gatteschi,* and C. Zanchini

Received March 6, 1980

We have recently started a program of characterization of the ESR spectra of high-spin cobalt(II) complexes and have found that octahedral[1,2] and square-pyramidal[3] complexes on one side and tetrahedral complexes[4,5] on the other side are very sensitive to low symmetry components of the ligand field. In all the reported cases, the ESR spectra could be interpreted by using an $S = {}^1/_2$ effective spin Hamiltonian. In particular tetrahedral complexes are characterized by g values ranging from 6.7 to 1.5, while square-pyramidal complexes can give g values higher and lower than these limits. Further the hyperfine splitting in tetrahedral complexes is in general small[6-8] so that often it is not resolved, while it tends to be larger in octahedral and square-pyramidal complexes. Trigonal-bipyramidal complexes have an orbitally nondegenerate ground state,[9,10] so that their ESR spectra should not be dissimilar from those of tetrahedral complexes. In order to verify if there is any possibility to discriminate between these two stereochemistries through ESR spectra, we wish to report here the ESR spectra of pentakis(picoline *N*-oxide)cobalt(II) perchlorate which has been shown to contain fairly regular trigonal-bipyramidal CoO_5 chromophores[11,12] and which has electronic spectra that have been characterized through a single-crystal polarized-light experiment.[12]

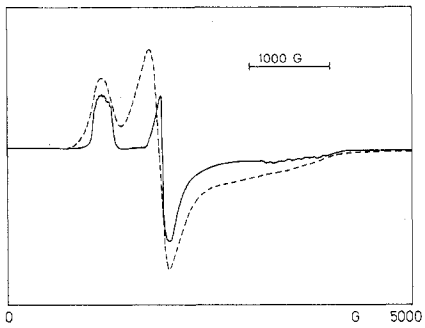

Figure 1. Polycrystalline powder ESR spectra of Co(picoline *N*-oxide)$_5$(ClO$_4$)$_2$ (---) and of (Zn,Co)(picoline *N*-oxide)$_5$(ClO$_4$)$_2$ (—) recorded at 4.2 K at X-band frequency, in the range 0–5000 G.

Table I. Principal g Values and Direction Cosines for Co(picoline *N*-oxide)$_5$(ClO$_4$)$_2$

g	crystallographic frame[a]			molecular frame[b]		
1.86 (3)	0.1825	0.1608	0.9700	0.1169	−0.0725	0.9905
3.53 (2)	0.9638	0.2245	0.1141	0.9904	−0.0662	−0.1217
5.67 (1)	0.1946	0.9611	−0.1960	0.0744	0.9951	0.0641

[a] The crystallographic frame is a^*bc. [b] The molecular frame is centered on the metal atom with z parallel to the Co–O$_2$ bond direction and x parallel to a projection of the Co–O$_3$ bond direction in the plane orthogonal to z.

Experimental Section

The cobalt and zinc derivatives were obtained from ethanolic solutions of stoichiometric amounts of picoline *N*-oxide and the perchlorate of the metals. The needlelike crystals of pure and diluted complexes were grown in butanolic solutions with triethyl orthoformate in a slow stream of dry nitrogen. They were oriented by the Weissenberg technique, according to a previous report.[12]

ESR spectra down to 4.2 K were recorded with the apparatus described elsewhere.[2]

(1) Part 6: Bencini, A.; Benelli, C.; Gatteschi, D.; Zanchini, C. *Inorg. Chem.* **1980**, *19*, 3027.
(2) Bencini, A.; Benelli, C.; Gatteschi, D.; Zanchini, C. *Inorg. Chem.*, in press.
(3) Bencini, A.; Benelli, C.; Gatteschi, D.; Zanchini, C. *Inorg. Chem.* **1979**, *18*, 2526.
(4) Bencini, A.; Gatteschi, D. *Inorg. Chem.* **1977**, *16*, 2141.
(5) Bencini, A.; Benelli, C.; Gatteschi, D.; Zanchini, C. *Inorg. Chem.* **1979**, *18*, 2137.
(6) Desideri, A.; Morpurgo, L.; Raynor, J. B.; Rotilio, G. *Biophys. Chem.* **1978**, *8*, 267.
(7) Kennedy, F. S.; Hill, H. A. D.; Kaden, T. A.; Vallee, B. L. *Biochem. Biophys. Res. Commun.* **1972**, *48*, 1533.
(8) Bencini, A.; Benelli, C.; Gatteschi, D.; Zanchini, C. *J. Mol. Struct.* **1980**, *60*, 401.
(9) Ciampolini, M.; Bertini, I. *J. Chem. Soc. A* **1968**, 2241.
(10) Wood, J. S. *Prog. Inorg. Chem.* **1972**, *16*, 227.
(11) Coyle, B. A.; Ibers, J. A. *Inorg. Chem.* **1970**, *9*, 767.
(12) Bertini, I.; Dapporto, P.; Gatteschi, D.; Scozzafava, A. *Inorg. Chem.* **1975**, *14*, 1639.

0020-1669/80/1319-3839$01.00/0